IAES International Journal of Artificial Intelligence (IJ-AI)
Vol. 15, No. 3, June 2026, pp. 2181~2191
ISSN: 2252-8938, DOI: 10.11591/ijai.v15.i3.pp2181-2191

Hybrid automated road crack segmentation using morphological operations and boundary tracing

Ida Ayu Ari Angreni[1], Diyanti[1], Vega Valentine[2]
[1]Department of Civil Engineering, Faculty of Civil Engineering and Planning, Gunadarma University, Depok, Indonesia
[2]Department of Informatics, Faculty of Industry Technology, Gunadarma University, Depok, Indonesia

Article Info

Article history:

Received Jul 12, 2025
Revised Apr 14, 2026
Accepted May 11, 2026

Keywords:

Contrast limited adaptive histogram equalization
Cracks
Deepcrack
Morphology
Pipeline

ABSTRACT

Cracks in the road surface are one of the early indicators of structural damage that has an impact on safety and infrastructure maintenance costs. Accurate early detection is a challenge in complex visual conditions such as uneven lighting and varied asphalt textures. This study proposes an efficient and fully automated hybrid segmentation method to detect cracks in road surface imagery. This method consists of several main stages: image enhancement using contrast limited adaptive histogram equalization (CLAHE), initial segmentation through a combination of Otsu's thresholding, adaptive Gaussian thresholding, and Canny edge detection, followed by mask enhancement with morphological operations (closing, opening, and erosion). The DeepCrack dataset is used as a source of test data. The evaluation results showed high performance with detection accuracy reaching 95.82%. These findings show that the proposed method is not only precise and sensitive, but also adaptive to visual variation without the need for manual training or parameters. A major novelty lies in the integration of three classic segmentation methods in one morphology pipeline that is computationally lightweight yet competitive, making it potential for real-world applications of automated inspection systems.

Corresponding Author:

Ida Ayu Ari Angreni
Department of Civil Engineering, Faculty of Civil Engineering and Planning, Gunadarma University
Margonda Raya 100, Pondok Cina, Depok, West Java, Indonesia
Email: idaayu@staff.gunadarma.ac.id

1. INTRODUCTION

Roads as the main transportation infrastructure play an important role in inter-regional connectivity and economic growth [1]. Good road surface quality greatly determines user safety, travel time efficiency, and smooth logistics distribution. However, over time, the road surface suffers damage characterized by the appearance of cracks, which can be caused by environmental factors such as extreme weather, as well as human factors such as repeated overload of traffic [2]. Such damage, if not detected and addressed early, can develop into potholes and exacerbate the degradation of road infrastructure, ultimately increasing the risk of accidents and maintenance costs. The process of monitoring road conditions conventionally still relies on manual inspections [3] which requires a lot of labor, cost, and time. The development of automated methods for detecting and analyzing cracks in road surfaces is an urgent need [4]. One promising approach is digital image processing, which allows the systematic and objective extraction of visual information from road surface images.

Various methods have been developed to detect cracks, ranging from conventional thresholding, edge detection, to machine learning-based approaches [5]. However, the main challenge that is still a significant obstacle is the irregularity of the shape of the crack [6], low contrast between cracks and background, as well as visual disturbances due to non-uniform lighting or complex asphalt surface textures [7]. Under these conditions, a single method often fails to produce precise segmentation, either due to errors in setting thresholds or inability to trace the contours of the crack in its entirety. Deep learning-based approaches are promising, but they tend to require large computing resources and complex training processes. An efficient, fully automated, and capable method is needed to accommodate complex visual variations of cracks [8] in field conditions. In this study, a hybrid approach was developed that integrates automatic Otsu thresholding, morphological operations, and boundary tracing techniques, which is designed to provide a more adaptive and computationally lightweight segmentation solution [9]. This combination not only improves segmentability in complex imaging conditions, but also maintains runtime efficiency, making it suitable for the practical and large-scale implementation of road inspection systems.

Research related to the detection and segmentation of cracks on road surfaces has been carried out a lot, both with a classical approach based on image processing and methods based on deep learning. However, most of these approaches still face significant obstacles in dealing with complex visual conditions, such as uneven lighting, varying surface textures, and irregular crack shapes. He *et al.* [10] developed a hybrid method of deformable oriented (DO)-YOLOv4-image processing techniques (IPTs), which combines detection using deformable convolutional YOLOv4 with segmentation based on classical IPTs. This method is able to improve detection accuracy and reduce the annotation load by up to 90%, but still relies on manual adjustment of segmentation parameters. Deng *et al.* [1] proposed a detection-segmentation-quantification framework using YOLOv5 and Res-UNet modifications, which proved effective in complex environments, but trials were still limited to large-scale cracks. Meanwhile, Ong *et al.* [11] offers a hybrid method of shortest distance and orthogonal projection-based crack width measurement, which excels in accuracy but is limited to pre-skeletonized imagery. In the context of semantic segmentation, knowledge transfer among the class activation maps and encoder–decoder segmentation network (KTCAM)-Net [12] demonstrate superior performance through the integration of class activation maps (CAM) with encoder-decoder, supported by hybrid loss functions and refinement boundaries, although the complexity of the architecture may limit real-time implementation. Tiwari *et al.* [13] combining features from improved pyramid scene parsing network (PSP-Net), holistically-nested edge detection (HED) network, and local binary pattern (LBP) for crack classification using XGBoost, achieving up to 99.09% accuracy, but with a computationally heavy multi-component system. All of these approaches show significant progress, but leave gaps in terms of efficiency, full automation, and adaptability to small-featured cracks in real-world conditions.

Chen *et al.* [14] proposes novel crack detection model based on multiple selective fusion (MSF-CrackNet), a network of encoders that is reinforced with several mechanisms selective fusion to overcome the challenges of crack segmentation in images with complex backgrounds, high noise, and fine cracks. The model was tested on three public datasets (SCD, CFD, and DeepCrack) and showed superior performance with a dice value of up to 86.8% and mean intersection over union (mIoU) of up to 87.9%, outperforming popular models such as U-Net and DeepLabv3+. The advantage of this method lies in the integration of star feature enhancement, adaptive fusion, and selective output modules designed to maintain local information, handle class imbalances, and reduce computational complexity.

All of the previously developed approaches show significant progress in road crack segmentation and analysis, but still leave a number of important limitations. Some advanced deep learning methods such as DO-YOLOv4-IPTs [10] and KTCAM-Net [12] offers high accuracy, but relies on parameters that must be manually adjusted or require complex architectures that are inefficient for real-time implementation, especially on devices with limited computing power. Although the results are promising, the limitations of the research [14] lies in the reliance on complex network structures and the lack of direct evaluation of the success of the deployment in real environments or low-spec edge devices. Other research such as that conducted by [1], [11] have not optimally accommodated the characteristics of small-scale cracks or image conditions with high noise and extreme texture variations, which are commonly found in real-world scenarios.

In this study, a road crack segmentation approach was developed that directly responds to the main challenges in infrastructure image detection, namely dependence on manual labeling, sensitivity to lighting, and computational complexity in modern models. Based on these gaps, this study designed a computationally lightweight yet adaptive segmentation pipeline, through the integration of Otsu's thresholding, morphology operation series, and boundary tracing in one fully automated system. The main novelty lies in the reorganization of classical techniques into a segmentation approach that is not only free of training parameters and manual adjustments, but also remains accurate in real image conditions containing noise, thin cracks, and non-uniform intensity. The urgency of this research is reinforced by the need for a crack detection system that is fast, resource-efficient, and can be applied to limited devices in the field such as unmanned aerial vehicles (UAVs) or edge devices, without losing accuracy or reliability.

2. METHOD

A hybrid method was developed in this study to address the challenges of road crack segmentation under complex visual conditions, such as uneven lighting, low contrast, and irregular crack shape. The segmentation process is carried out through the pre-processing stages of imagery, automatic thresholding using the Otsu method, morphological operations, and object boundary tracking with boundary tracing. Each stage is structured in an integrated manner to produce precise and efficient crack segmentation without the need for manual adjustments.

2.1. DeepCrack dataset

This study uses the public DeepCrack dataset [15], which consists of 537 RGB road crack images with a resolution of 544×384 pixels and manually annotated binary masks. The dataset is divided into 300 training images and 237 testing images, containing various crack scales, lighting conditions, shadows, textures, and noise. The crack widths range from 1 pixel to more than 180 pixels, making the dataset challenging for crack segmentation tasks.

2.2. Preprocessing of road damage images

Image preprocessing is a very important first step in the process of analyzing road damage images. In this study, preprocessing was carried out to improve the quality of the image and prepare it to be suitable for further analysis. This process includes a series of methods that aim to eliminate distractions, adjust the size, as well as extract important features from the image. The algorithms used in this stage include:

i) Converts RGB imagery from road surface, to grayscale imagery: this conversion is done because intensity-based segmentation is simpler in one luminance channel than in three color channels. This process is done using (1) [16].

$$I_{gray}(x,y) = 0.299R(x,y) + 0.587G\ (x,y) + 0.114\ B(x,y) \tag{1}$$

Variable $I_{gray}(x,y)$ is the standard equation for converting color imagery (RGB) to grayscale imagery. Every pixel (x,y) in grayscale imagery obtained from a linear combination of red (R), green (G), and blue (B) intensity values at the same pixel, with a weight that reflects the sensitivity of the human eye to each color channel. Green canals have the largest contribution of 0.587 because the human eye is most sensitive to green [17], followed by red at 0.299, and blue at 0.114 which had the least effect. The result of this conversion results in a single-channel image with a grayness level between 0 (black) to 255 (white), and is used as a basis in the segmentation process because it is more efficient to analyze compared to three-channel imagery.

ii) Setting the distribution of grayscale image histograms of road damage: this stage is the first step in the contrast limited adaptive histogram equalization (CLAHE) algorithm, which serves to adjust the distribution of histogram so that it does not overcontrast or accentuate excessive noise, using (2) [18].

$$h_{clipped}(i) = \min\ [h(i), T \tag{2}$$

$h(i)$ expresses the intensity histogram value at level I (in the range 0–255) on a single small block (tile) of the grayscale image of the road damage. Meanwhile, T is the clip limit value, which is the maximum limit of the number of pixels allowed for each intensity level. If a histogram value h(i) exceeding the threshold value T, then the value will be cut to T. This means that a very high histogram (an indication of extreme contrast or dominant noise) will be "trimmed" so that the distribution peaks are not too sharp. This process is called clipping [19].

iii) Maintain a balance of pixel distribution: after the histogram the intensity is trimmed with a clip limit. This stage is important to maintain a balance of pixel distribution across the intensity range without drastically losing information. After the histogram of each tile is cut using $h_{clipped}(i)$, then there will be a number of pixel surplus from intensity levels that initially exceed the threshold [20]. The total amount of this excess is referred to as the excess, which is calculated using (3).

$$excess = \sum_i (h(i) - T) \tag{3}$$

All the differences between the original histogram h(i) and the maximum value T in (3) are added to get how many pixels are "truncated". The next step is to distribute this excess evenly across all existing intensity levels (bins). If there are N total bins (usually 256 for an 8-bit image), then each bin will get an additional value of Δ as many as (4).

$$\Delta = \frac{excess}{N} \tag{4}$$

The histogram that has been cut out earlier is updated to histogram that has been redistributed using (5).

$$h'(i) = h_{clipped}(i) + \Delta \quad (5)$$

All image information is retained but in a more even distribution and not excessively at one or two levels of intensity. This step plays an important role so that the application of equalization histograms is local but stable, so that cracks or small details in the image remain clearly visible after contrast processing [21].

iv) Calculating the cumulative distribution function (CDF): the CDF of the histogram that has been modified in this study uses (6) [22].

$$CDF\ (i) = \sum_{k=0}^{i} h'(k) \quad (6)$$

This stage is a pixel intensity transformation process, where the CDF value at the i-th intensity level indicates the total number of pixels from intensity level 0 to i. The greater the value i, the more pixels are collected in this accumulation. This stage is used to ensure that the output value of the equalization result is within the specified intensity range (0–255) [23].

v) Perform intensity mapping in the CLAHE algorithm using (7).

$$I_{out}\ (x, y) = CDF\ \left(I_{gray}(x, y)\right) x\ 255 \quad (7)$$

The preprocessing stage began by converting the RGB road image into a grayscale image to simplify intensity analysis. Contrast enhancement was then performed using CLAHE with a clip limit of 4.0 and a tile grid size of 8×8. This process improved local contrast and enhanced crack visibility under varying illumination conditions.

2.3. Crack detection

Once the preprocessing is complete and the image contrast has been enhanced, the next step is to detect the crack regions in the road surface. The first stage of detection involves automated global segmentation using Otsu Thresholding. This method generates a binary mask by calculating an optimal threshold that separates the background from the crack regions in the grayscale image. The process involves computing the histogram of pixel intensities, determining the threshold value that minimizes intra-class variance, and applying binarization to produce a clear distinction between cracks and the background, ensuring accurate segmentation for further analysis as in (8) and (9).

i) Perform automated global segmentation. Segmentation is done using Otsu thresholding to generate a binary image (mask) of the grayscale based on an automatic threshold that separates the background and the crack object globally [24]. This segmentation is carried out in stages: calculating the histogram, finding the threshold, and binarization.
   – Calculating the h(i) histogram of a grayscale image
   – Find the threshold value t that minimizes intra-class variance using (8).

$$\sigma_w^2(t) = \omega_0(t)\sigma_0^2(t) + \omega_1(t)\sigma_1^2(t) \quad (8)$$

Where and is the probability of pixels below and above the threshold t. The optimal t threshold is used for binarization using (9): $\omega_0(t)\sigma_0^2(t)\omega_1(t)\sigma_1^2(t)$.

$$I_{otsu}\ (x, y) = \begin{cases} 255,\ Jika\ I_{gray}(x, y) > t \\ 0,\ Jika\ I_{gray}(x, y) \leq t \end{cases} \quad (9)$$

ii) Detecting locally sensitive light. To capture cracks that may be missed by global segmentation, locally adaptive thresholding is applied using a Gaussian method. This approach computes a weighted average of pixel intensities within a local window and adjusts the threshold using a constant C to account for uneven lighting conditions. As a result, faint cracks and areas with variable illumination are effectively detected, complementing the global segmentation step and improving overall detection accuracy (10). This process is carried out using adaptive thresholding Gaussian to capture local crack patterns that may not be detected by Otsu, especially in uneven lighting areas [25], as follows:
For each pixel (x,y) grab the W×W local window.
Calculate the weighted average of neighbor intensities using the Gaussian kernel [26].
Reduce the result by constant C to set the sensitivity.
Apply a local threshold using (10).

$$I_{adapt}(x,y) = \begin{cases} 255, \ Jika \ I_{gray}(x,y) > \mu_G(x,y) - C \\ 0, \ Others \end{cases} \quad (10)$$

$\mu_G(x,y)$ are a local Gaussian mean and a constant C. It is usually set to 3-10 so that it is not too sensitive to noise [27].

iii) Sharpening the edge of the crack: after thresholding, the edges of the cracks are sharpened using Canny edge detection to ensure precise and smooth edge detection. This stage begins with noise reduction using a Gaussian blur, followed by calculating horizontal and vertical gradients using the Sobel operator. The gradient magnitude and direction are then determined (11), and non-maximum suppression is applied to thin the edges. A double threshold distinguishes strong and weak edges, and edge tracking ensures that only weak edges connected to strong edges are preserved, resulting in clean and continuous crack boundaries. Detecting crack edges must be done precisely and smoothly, especially on fine line structures that are difficult to capture ordinary thresholds. This study uses Canny edge detection with the following stages:
Stage 1. Reduce noise using Gaussian blur [28].
Stage 2. Detects horizontal and vertical edges with Sobel gradient [29].
Stage 3. Count magnitude and gradient direction using (11) [30].

$$G = \sqrt{G_x^2 + G_y^2}, \theta = tan^{-1}\left(\frac{G_y}{G_x}\right) \quad (11)$$

Stage 4. Thinning edges using non-maximum suppression [31].
Stage 5. Double threshold with the following conditions:
– Strong Edge If G > Thigh
– Weak Edge If Tlow <G ≤ Thigh
Stage 6. Tracking the edge of the road crack where only the weak edge connected to the strong edge will be maintained

The outputs from Otsu thresholding, adaptive Gaussian thresholding, and Canny edge detection were combined using bitwise OR operations to generate a comprehensive crack mask. This integration enables the detection of crack regions that may not be captured by a single method alone. The resulting binary mask was then used for morphological refinement and boundary tracing.

2.4. Binary mask incorporation

After obtaining the initial detection results from Otsu thresholding, adaptive Gaussian thresholding, and Canny edge detection, the next step is to combine these outputs to form a more comprehensive crack mask. The combination is performed using a pixel-wise OR operation, ensuring that cracks detected by any of the three methods are included in the merged mask as in (12) [32]. This approach enhances the robustness of crack detection by covering patterns that may be missed by individual methods.

$$Mask_{mix}(x,y) = otsu(x,y) \ \cup Adaptive\ (x,y)\ \cup Canny\ (x,y) \quad (12)$$

This step aims to unify the detection power of all three methods, so that crack patterns that may not be captured by one method can be covered by another. The combined mask results are then refined using a series of morphological operations aimed at cleaning the noise and correcting the shape of the cracks, with the following:

i) The combined mask is then refined using morphological operations to remove noise and correct the shape of detected cracks. First, a closing operation is applied, which consists of dilation followed by erosion using a structural element B, as shown in (13). The structural element is a small binary matrix, where 1 indicates an active pixel influencing the operation and 0 is ignored. By sliding this element over the binary image, small gaps and broken crack lines are closed, improving the continuity of detected crack patterns.

$$Mask_{close} = (Mask_{mix} \oplus B) \ominus B \quad (13)$$

The structure of element B is a small matrix containing binary values (0 and 1) that are used as local filters in morphology. A value of 1 indicates an active pixel that will affect the operation, while 0 is ignored. The structure of these elements is "shifted" (moved) throughout the binary image to apply operations such as dilation (⊕) or erosion (⊖), to determine the overlap between element 1 on B and the foreground pixel (white) on the image. This operation serves to close small gaps or broken crack lines.

ii) Next, an opening operation is applied, which consists of erosion followed by dilation, and is often repeated with additional erosion to remove oversegmented or excessively thick regions as in (14) and (15). This step also eliminates small irrelevant objects such as single-pixel noise or background fragments. Reapplying the opening operation at the final stage further smooths the shape of the cracks, resulting in a cleaner and more precise segmentation mask that is ready for the subsequent boundary tracing or contour analysis stage.

$$Mask_{open} = (Mask_{close} \ominus B) \oplus B \tag{14}$$

iii) After erosion, redoing the opening is useful for removing small irrelevant objects such as single-pixel noise or small fragments from the background. Erosion operations are performed using (15).

$$Mask_{erode} = Mask_{open} \ominus B \tag{15}$$

The masks generated from Otsu thresholding, adaptive Gaussian thresholding, and Canny edge detection were combined using bitwise OR operations. Morphological refinement was then applied using a 5×5 elliptical structuring element. The refinement process consisted of closing operations to fill small gaps and connect crack regions, followed by opening operations to remove noise and smooth object boundaries. An additional erosion step was applied to suppress remaining artifacts. A final opening operation was performed to further refine the crack shape and improve segmentation clarity. These operations produced a cleaner and more precise crack segmentation mask for the subsequent boundary tracing stage.

3. RESULTS AND DISCUSSION

This section presents the results of the implementation of the methods that have been developed as well as a discussion of the performance of road damage image segmentation based on the stages of preprocessing, crack detection, mask merger, and morphology refinement. Evaluation was carried out on the visual quality of the segmentation results as well as the calculation of quantitative metrics such as precision, recall, F1-score, intersection over union (IoU), and accuracy. Each stage of image processing is visually displayed to show the contribution of each method in improving the clarity and accuracy of the detected crack area. The results of this experiment aim to validate the effectiveness of the proposed hybrid approach, particularly in dealing with cracks with complex morphologies as well as non-uniform lighting conditions on the road surface.

3.1. Road damage image preprocessing results

Figure 1 shows the overall results of the road damage image preprocessing stage using CLAHE enhancement. Figure 1(a) shows the initial image in grayscale with no increased contrast where after preprocessing the CLAHE result image is produced in Figure 1(b) showing previously faint details becoming sharper and cracks more visible. The distribution of pixel intensity values before and after CLAHE is shown in Figure 1(c). CLAHE spreads the intensity values more evenly than the original histogram, which is usually concentrated in a certain range. The cumulative curve of pixel distribution is shown in Figure 1(d) as a CDF curve that shows a more linear and even transition, reflecting an effective local contrast increase. This stage shows that CLAHE not only improves the visual quality of the image locally, but also balances the intensity distribution statistically, which is very beneficial for the next stage of crack segmentation.

3.2. Combined mask results

Figure 2 shows the visual results of the morphological operation series applied to the combined crack detection mask. Figure 2(a) shows the results of the closing operation, namely a combination of dilation followed by erosion using a disk-shaped element structure. This operation successfully closes small gaps and connects the parts of the cracks that were previously severed, so that the crack area becomes more intact and united. Next, Figure 2(b) shows the results of the opening operation, namely erosion followed by dilation. This process is effective in removing small noises or foreign objects outside the crack area, especially small irrelevant dots or debris. Finally, Figure 2(c) shows the results after the application of additional erosion operations, which serve to erode the edges of the object and reduce oversegmentation in areas that are too thick. The combination of these three operations as a whole results in a smoother, cleaner crack mask that focuses on the main structure of the crack, thus improving accuracy in the final segmentation and contour tracking stages.

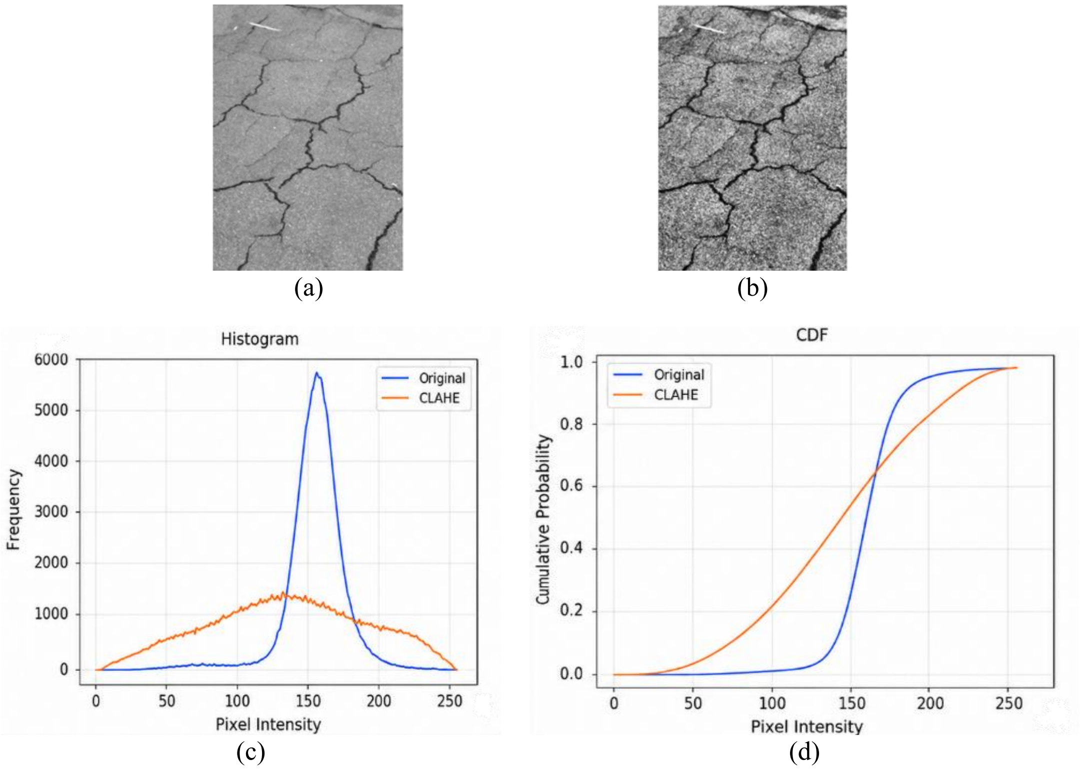

Figure 1. Road damage image preprocessing results: (a) original grayscale image, (b) CLAHE output, (c) pixel intensity histogram before and after enhancement, and (d) CDF curve after preprocessing

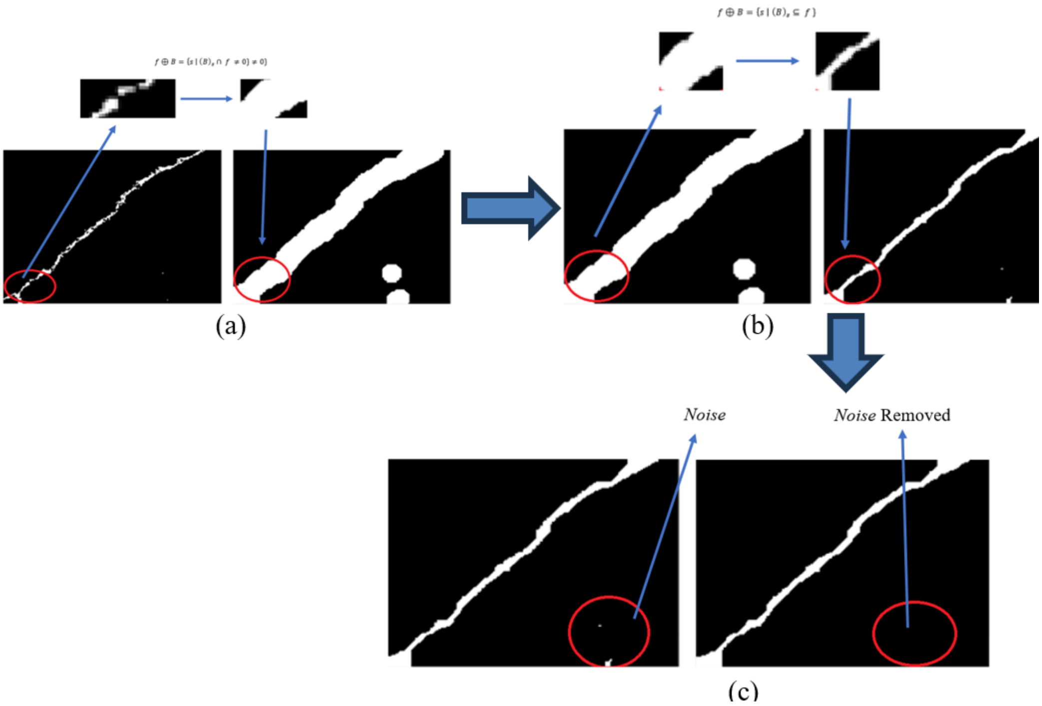

Figure 2. Binary mask incorporation stage: (a) closing operation, (b) opening operation, and (c) erosion operation

3.3. Segmentation results with Otsu's thresholding

Adaptive Gaussian thresholding was applied to overcome the limitations of global thresholding under uneven illumination conditions. The method successfully captured thin and low-contrast crack patterns that were not consistently detected by Otsu thresholding. However, the approach was more sensitive to variations in road surface texture, which occasionally produced false detections in non-crack regions. Despite this limitation, adaptive Gaussian thresholding improved segmentation sensitivity and contributed to more comprehensive crack extraction when combined with other segmentation techniques. The crack detection stage plays a crucial role in the segmentation pipeline by identifying crack patterns accurately and comprehensively from road surface images. To address challenges such as non-uniform illumination, complex textures, and irregular crack structures, a hybrid segmentation approach was implemented using Otsu thresholding, adaptive Gaussian thresholding, and Canny edge detection. Otsu thresholding provided global binary segmentation based on image intensity, while adaptive Gaussian thresholding enhanced local crack detection in regions with varying illumination. In addition, Canny edge detection was employed to identify fine crack boundaries with high precision.

The outputs generated by these three techniques were combined using a bitwise OR operation to produce a more robust and comprehensive binary crack mask. This integration allowed each method to complement the limitations of the others, thereby improving the overall segmentation quality. The segmentation results and the final combined mask are presented in Figure 3, demonstrating the effectiveness of the proposed approach in extracting crack features under challenging visual conditions.

The resulting segmentation mask served as the basis for subsequent morphological refinement and boundary tracing processes. The segmentation performance of the proposed system was evaluated using standard performance metrics to assess the accuracy and completeness of crack detection. As illustrated in Figure 4, the proposed hybrid approach achieved consistent segmentation performance across various road surface conditions. These results demonstrate that the integration of global thresholding, local adaptive thresholding, and edge-based detection techniques provides a robust and reliable solution for automated road crack segmentation.

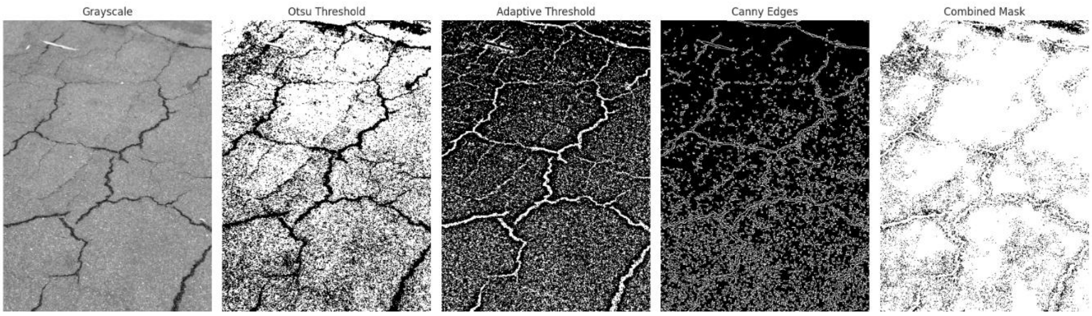

Figure 3. Results of road crack segmentation

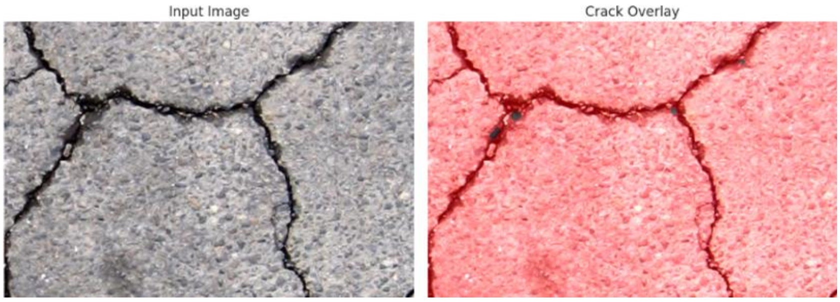

Figure 4. Road damage image overlay

The proposed hybrid segmentation approach achieved strong performance across all evaluation metrics. A precision value of 0.8579 indicates that most detected crack regions were correctly classified, while the recall value of 1.0000 demonstrates that the system successfully identified all crack regions in the ground truth without false negatives. The F1-score of 0.9235 reflects a balanced performance between precision and recall, confirming the effectiveness of the proposed method in detecting both prominent and fine crack structures. In addition, the IoU value of 0.8579 indicates a high level of agreement between the predicted segmentation and the ground truth mask. The overall accuracy reached 0.9582, showing that the majority of image pixels were correctly classified as crack or background. These results demonstrate that the proposed approach provides accurate, robust, and reliable crack segmentation under complex road surface conditions.

3.4. Comparison with previous studies and performance evaluation

Table 1 presents a comparative overview of representative prior studies on road crack segmentation, highlighting their methodologies, datasets, key performance metrics, and associated advantages or limitations. Traditional hybrid approaches such as DO-YOLOv4-IPTs [10] achieve moderate accuracy (~90%) but require manual parameter adjustment, limiting their practical applicability. Similarly, KTCAM-Net [12], despite slightly higher accuracy (~92%), relies on complex encoder-decoder architectures that are computationally intensive and slow for real-time deployment. More recent networks, such as MSF-CrackNet [14], demonstrate high segmentation performance on public datasets (Dice 86.8%, mIoU 87.9%) through multi-selective fusion strategies, yet demand significant computational resources.

In contrast, the proposed study demonstrates competitive quantitative performance while introducing several key novelties. First, the approach is fully automated, eliminating the need for manual threshold tuning or parameter adjustment. Second, it is computationally lightweight, combining classical IPTs: Otsu thresholding, adaptive Gaussian thresholding, Canny edge detection, and morphology operations, into an integrated pipeline suitable for real-time or edge-device deployment. Third, it exhibits robustness to faint, irregular, and complex crack patterns under varying lighting and surface conditions, addressing limitations observed in both classical and deep learning-based methods.

Table 1. Comparison of current study with previous research

Study	Method	Dataset	Key metrics	Advantage / Limitation
DO-YOLOv4-IPTs [10]	Hybrid YOLOv4 + Classical	Road images	Accuracy ~90%	Needs manual adjustment
KTCAM-Net [12]	CAM-based encoder-decoder	Road images	Accuracy ~92%	Complex, slow
MSF-CrackNet [14]	Multi-selective fusion network	SCD/CFD/DeepCrack	Dice 86.8%, mIoU 87.9%	High performance, resource intensive
Proposed study	Otsu + adaptive Gaussian + Canny + morphology	Road images	F1-score 0.9235, IoU 0.8579, Accuracy 0.9582	Fully automated, lightweight, robust to faint cracks

4. CONCLUSION

The hybrid segmentation method developed in this study, which combines Otsu's thresholding, adaptive Gaussian thresholding, and Canny edge detection and refined with morphological operations, has been shown to be effective in detecting and segmenting cracks on road surfaces with complex morphology and non-uniform lighting conditions. The evaluation results showed high performance with a precision of 0.8579, a recall of 1.0000, an F1-score of 0.9235, an IoU of 0.8579, and an overall accuracy of 0.8582, which confirms the system's level of accuracy and sensitivity in recognizing fine cracks as well as large cracks. Nonetheless, further development is still needed, especially in terms of data labeling automation, post-segmentation enhancements to reduce noise, and testing of more varied field imagery. In addition, future research directions can be focused on real-time application using lightweight edge devices to support efficient and portable road inspection systems.

ACKNOWLEDGMENTS

The authors would like to express their sincere gratitude to the Ministry of Higher Education, Science, and Technology of the Republic of Indonesia (Kemdiktisaintek) and the Research Directorate of Gunadarma University for their continuous support and facilitation throughout this research.

FUNDING INFORMATION

This research was funded by the penelitian fundamental regular under the Ministry of Higher Education, Science, and Technology of the Republic of Indonesia based on the decree of the Director of Research and Community Service no. 0419/C3/DT.05.00/2025 at May 22, 2025. This work was supported through main contract no. 124/C3/DT.05.00/PL/2025 at May 28, 2025, derivative contract no. 0974/LL3/AL.04/2025 at June 4, 2025, and derivative contract no. 16.17/LP/UG/VI/2025 at June 5, 2025.

AUTHOR CONTRIBUTIONS STATEMENT

This journal uses the Contributor Roles Taxonomy (CRediT) to recognize individual author contributions, reduce authorship disputes, and facilitate collaboration.

Name of Author	C	M	So	Va	Fo	I	R	D	O	E	Vi	Su	P	Fu
Ida Ayu Ari Angreni	✓	✓	✓	✓	✓	✓	✓	✓	✓	✓	✓	✓	✓	✓
Diyanti		✓	✓			✓		✓		✓				
Vega Valentine	✓			✓	✓					✓			✓	✓

C : **C**onceptualization
M : **M**ethodology
So : **So**ftware
Va : **Va**lidation
Fo : **Fo**rmal analysis
I : **I**nvestigation
R : **R**esources
D : **D**ata Curation
O : Writing - **O**riginal Draft
E : Writing - Review & **E**diting
Vi : **Vi**sualization
Su : **Su**pervision
P : **P**roject administration
Fu : **Fu**nding acquisition

CONFLICT OF INTEREST STATEMENT

Authors state no conflict of interest.

INFORMED CONSENT

This study did not involve human participants; therefore, informed consent was not required.

ETHICAL APPROVAL

This study utilized pest dataset and did not involve human or vertebrate animal subjects; therefore, ethical approval was not required.

DATA AVAILABILITY

This study uses road damage imagery data obtained from DeepCrack, a widely used and reputable public dataset in the study of crack detection and segmentation on road surfaces. This dataset is publicly available in GitHub at https://github.com/qinnzou/DeepCrack link, thus allowing replication of the data collection process by other researchers. Detailed descriptions of the data preprocessing procedures, image selection criteria, and variable transformations applied in this study can be obtained through a request to the corresponding author.

REFERENCES

[1] L. Deng, A. Zhang, J. Guo, and Y. Liu, "An integrated method for road crack segmentation and surface feature quantification under complex backgrounds," *Remote Sensing*, vol. 15, no. 6, Mar. 2023, doi: 10.3390/rs15061530.

[2] S. Bouhsissin, H. Assemlali, and N. Sael, "Enhancing road safety: a convolutional neural network based approach for road damage detection," *Machine Learning with Applications*, vol. 20, Jun. 2025, doi: 10.1016/j.mlwa.2025.100668.

[3] X. Yang, J. Zhang, W. Liu, J. Jing, H. Zheng, and W. Xu, "Automation in road distress detection, diagnosis and treatment," *Journal of Road Engineering*, vol. 4, no. 1, pp. 1–26, Mar. 2024, doi: 10.1016/j.jreng.2024.01.005.

[4] P. M. S. Raihan *et al.*, "Pavement crack detection and solution with artificial intelligence," *European Journal of Theoretical and Applied Sciences*, vol. 2, no. 4, pp. 277–314, Jul. 2024, doi: 10.59324/ejtas.2024.2(4).25.

[5] F. Şermet and I. Pacal, "Deep learning approaches for autonomous crack detection in concrete wall, brick deck and pavement," *Dicle University Journal of Engineering*, vol. 15, no. 2, pp. 503–513, Apr. 2024, doi: 10.24012/dumf.1450640.

[6] Y. Wu, S. Li, J. Li, Y. Yu, J. Li, and Y. Li, "Deep learning in crack detection: a comprehensive scientometric review," *Journal of Infrastructure Intelligence and Resilience*, vol. 4, no. 3, Sep. 2025, doi: 10.1016/j.iintel.2025.100144.

[7] M. Pal, P. Palevičius, M. Landauskas, U. Orinaitė, I. Timofejeva, and M. Ragulskis, "An overview of challenges associated with automatic detection of concrete cracks in the presence of shadows," *Applied Sciences*, vol. 11, no. 23, 2021, doi: 10.3390/app112311396.

[8] N. Hütten, M. A. Gomes, F. Hölken, K. Andricevic, R. Meyes, and T. Meisen, "Deep learning for automated visual inspection in manufacturing and maintenance: a survey of open-access papers," *Applied System Innovation*, vol. 7, no. 1, 2024, doi: 10.3390/asi7010011.

[9] Q. Yuan, Y. Shi, and M. Li, "A review of computer vision-based crack detection methods in civil infrastructure: progress and challenges," *Remote Sensing*, vol. 16, no. 16, Aug. 2024, doi: 10.3390/rs16162910.

[10] Z. He, C. Su, and Y. Deng, "A novel hybrid approach for concrete crack segmentation based on deformable oriented-YOLOv4 and image processing techniques," *Applied Sciences*, vol. 14, no. 5, Feb. 2024, doi: 10.3390/app14051892.

[11] J. C. H. Ong, M.-Z. P. Ismadi, and X. Wang, "A hybrid method for pavement crack width measurement," *Measurement*, vol. 197, Jun. 2022, doi: 10.1016/j.measurement.2022.111260.

[12] Z. Al-Huda, B. Peng, R. N. A. Algburi, M. A. Al-antari, R. AL-Jarazi, and D. Zhai, "A hybrid deep learning pavement crack semantic segmentation," *Engineering Applications of Artificial Intelligence*, vol. 122, Jun. 2023, doi: 10.1016/j.engappai.2023.106142.

[13] S. Tiwari, V. Somesh, R. V. Joshi, and G. P. Sharma, "A multi-scale hybrid segmentation and MRMR feature selection approach for road crack detection using XGBoost classifier," *International Journal of Intelligent Engineering and Systems*, vol. 18, no. 3, pp. 388–401, Apr. 2025, doi: 10.22266/ijies2025.0430.27.

[14] Y. Chen, T. Yang, S. Dong, L. Wang, B. Pei, and Y. Wang, "Enhancing crack segmentation network with multiple selective fusion mechanisms," *Buildings*, vol. 15, no. 7, Mar. 2025, doi: 10.3390/buildings15071088.

[15] Q. Zou, Z. Zhang, Q. Li, X. Qi, Q. Wang, and S. Wang, "DeepCrack: learning hierarchical convolutional features for crack detection," *IEEE Transactions on Image Processing*, vol. 28, no. 3, pp. 1498–1512, Mar. 2019, doi: 10.1109/TIP.2018.2878966.

[16] D. Wan, R. Lu, B. Hu, S. Shen, T. Xu, and X. Lang, "OTM-fusion: an image preprocessing method for object detection in grayscale image," *SSRN Electronic Journal*, 2023.
[17] M. Pourbakht and Y. Kametani, "A correlation between color preferences and virtual environment," *Journal of Cyberspace Studies*, vol. 9, no. 2, pp. 289–311, 2025, doi: 10.22059/jcss.2025.391822.1135.
[18] T.-W. Kuan *et al.*, "Improved AH2E2 contrast enhancement for deep learning on night-scenario canal segmentation," in *Frontiers in Artificial Intelligence and Applications*, Mar. 2025, pp. 134–143, doi: 10.3233/FAIA250115.
[19] F. Zhao, Y. Chao, and L. Li, "A crack segmentation model combining morphological network and multiple loss mechanism," *Sensors*, vol. 23, no. 3, Jan. 2023, doi: 10.3390/s23031127.
[20] A. Fawzi, A. Achuthan, and B. Belaton, "Adaptive clip limit tile size histogram equalization for non-homogenized intensity images," *IEEE Access*, vol. 9, pp. 164466–164492, 2021, doi: 10.1109/ACCESS.2021.3134170.
[21] R. M. Dyke and K. Hormann, "Histogram equalization using a selective filter," *The Visual Computer*, vol. 39, no. 12, pp. 6221–6235, Dec. 2023, doi: 10.1007/s00371-022-02723-8.
[22] L. Yang, J. Deng, H. Duan, and C. Yang, "An efficient semantic segmentation method for road crack based on EGA-UNet," *Scientific Reports*, vol. 15, no. 1, Sep. 2025, doi: 10.1038/s41598-025-01983-3.
[23] Y.-Y. Bae, D.-J. Cho, and K.-H. Jung, "A new log-transform histogram equalization technique for deep learning-based document forgery detection," *Symmetry*, vol. 17, no. 3, Mar. 2025, doi: 10.3390/sym17030395.
[24] X. Liu, L. Zhu, Y. Wang, and Z. Yu, "A crack detection system of subway tunnel based on image processing," *Measurement and Control*, vol. 55, no. 3–4, pp. 164–177, Mar. 2022, doi: 10.1177/00202940211062015.
[25] C. Chen, H. Seo, C. Jun, and Y. Zhao, "A potential crack region method to detect crack using image processing of multiple thresholding," *Signal, Image and Video Processing*, vol. 16, no. 6, pp. 1673–1681, Sep. 2022, doi: 10.1007/s11760-021-02123-w.
[26] J. Xing, P. Yang, and L. Qingge, "Robust 2D Otsu's algorithm for uneven illumination image segmentation," *Computational Intelligence and Neuroscience*, vol. 2020, pp. 1–14, Aug. 2020, doi: 10.1155/2020/5047976.
[27] I. Baglaeva, B. Iaparov, I. Zahradník, and A. Zahradníková, "Analysis of noisy transient signals based on Gaussian process regression," *Biophysical Journal*, vol. 122, no. 3, pp. 451–459, Feb. 2023, doi: 10.1016/j.bpj.2023.01.003.
[28] J. Noh, J. Jang, J. Jo, and H. Yang, "Crack segmentation using U-Net and transformer combined model," *Applied Sciences*, vol. 15, no. 19, Oct. 2025, doi: 10.3390/app151910737.
[29] S. Gupta, H. Singh, and Y. J. Singh, "Comprehensive study on edge detection," in *Proceedings of the NIELIT's International Conference on Communication, Electronics and Digital Technology (NICE-DT 2023)*, Singapore: Springer, 2023, pp. 445–462, doi: 10.1007/978-981-99-1699-3_30.
[30] D. Shojaei, P. Jafary, and Z. Zhang, "Mixed reality-based concrete crack detection and skeleton extraction using deep learning and image processing," *Electronics*, vol. 13, no. 22, Nov. 2024, doi: 10.3390/electronics13224426.
[31] M. Shahin, F. F. Chen, M. Maghanaki, A. Hosseinzadeh, N. Zand, and H. K. Koodiani, "Improving the concrete crack detection process via a hybrid visual transformer algorithm," *Sensors*, vol. 24, no. 10, May 2024, doi: 10.3390/s24103247.
[32] J. Luo, H. Lin, X. Wei, and Y. Wang, "Adaptive Canny and semantic segmentation networks based on feature fusion for road crack detection," *IEEE Access*, vol. 11, pp. 51740–51753, 2023, doi: 10.1109/ACCESS.2023.3279888.

BIOGRAPHIES OF AUTHORS

Ida Ayu Ari Angreni is a researcher, lecturer, and head of Institute of Research for Civil Engineering and Architecture at Gunadarma University. From 2013 until now has won 4 research grants from Higher Education, Research, and Technology of the Republic of Indonesia (RISTEKDIKTI). She published a book in 2022 on construction management, has 25 publications since 2012, as well as 3 intellectual property rights (IPR) since 2020. She can be contacted at email: idaayu@staff.gunadarma.ac.id.

Diyanti is currently a lecturer and researcher at Gunadarma University, has actively participated in research since 2009, with 40 published articles and 3 books in the field of on civil engineering, specifically on transportation infrastructure and water resources. She has also registered 8 IPRs since 2023. She can be contacted at email: diyanti@staff.gunadarma.ac.id.

Vega Valentine is a lecturer, researcher, and staff of Institute of Research in Gunadarma University. She has contributed in some research grants from Higher Education, Research, and Technology of the Republic of Indonesia (RISTEKDIKTI) since 2014, also actively contributing in joint community service with Museum Tekstil (2016) and Museum Kebaharian Jakarta since 2021. From 2012, she has 20 publications, 3 IPRs, and is currently continuing her participation in researches and community services. She can be contacted at email: valentine@staff.gunadarma.ac.id.